Jordan Journal of Civil Engineering, Volume **14**, No. **4**, **2020**

Synergistic Effects of Water Binder Ratio and Silica Fume on Permeability of High-Performance Concrete

Sanjay Kumar [1] ***and Baboo Rai*** [2]*

[1] Assistant Professor, Department of Civil Engineering, National Institute of Technology, Patna, India 800005. E-Mail: sanjay@nitp.ac.in
[2] Associate Professor, Department of Civil Engineering, National Institute of Technology, Patna, India 800005.
* Corresponding Author. E-Mail: baboo.rai@nitp.ac.in; ORCiD Id- 0000-0001-6692-2241.

ABSTRACT

Ingress of water or permeation is difficult to measure as the quality of concrete increases. In the case of High-Performance Concrete (HPC), it becomes more difficult. In HPC, the concrete skeleton becomes so dense that the measurement of water permeability procedure becomes very precise and accurate. HPC is broadly utilized to enhance the durability and performance of structures, but there are few test procedures ready to assess its permeability-related properties. In this study, compressive strength, ultrasonic pulse velocity (UPV) and water permeability of HPC with silica fume were measured. The experimental results revealed that compressive strength, as well as pulse velocity of concrete, increased with the increase in silica fume content at the same w/c ratio. A mathematical model is presented for estimating the compressive strength of high-strength concrete incorporating silica fume. Subsequently, the synergistic effects of w/c ratio and silica fume (SF) on compressive strength, UPV and water permeability are statistically evaluated. This paper presents experimentally-based models with high coefficients of correlation in predicting the permeability and strength of HPC as a function of mixture design parameters (water-binder ratio and %SF). Contour diagrams to facilitate the use of the models are also established.

KEYWORDS: Silica fume, Compressive strength, Permeability, UPV, Contour plots.

INTRODUCTION

There are two basic conditions for avoiding leaks from a concrete containment structure: minimum concrete permeability and prevention of building defects. This paper is mainly concerned with the intrinsic permeability of concrete, but the selection process for concrete mixes required consideration of building factors, such as placeability. An important parameter for evaluating the durability performance and service life of an existing concrete structure is permeability (Chia & Zhang, 2002; Salvoldi, Beushausen & Alexander, 2015; Zunino & Lopez, 2016).

Permeability, absorption and sorptivity are the properties related to permeation, which primarily control the penetration of aggressive substances into the concrete. Permeability is defined as the coefficient representing "the rate at which water is transmitted through a saturated specimen of concrete under an externally maintained hydraulic gradient". It is well accepted that permeability is a good indicator, as it is inversely linked to durability (Bentz, Ehlen, Ferraris & Garboczi, 2001).

It is known that permeability controls deterioration of concrete in an aggressive environment. This is because the transport processes in concrete govern the deterioration processes, like carbonation, chloride attack and sulfates attack. Improvement in strength and other properties of concrete is due to the fillers and pozzolanic materials introduced to the concrete mix (Aitcin, Sarkar & Laplante, 1990). The ingress of moisture and aggressive ions is reduced due to the use of blended cement or supplementary cementing materials (SCMs). Therefore, the blending of Portland cement with other

Received on 16/8/2019.
Accepted for Publication on 9/7/2020.

pozzolanic materials has become a recognized technique in the construction of structures exposed to harsh environments.

With the advent of superplasticizer in the 1970s, it has become relatively simple to produce concrete with a compressive strength greater than 50 MPa. At the same time, the demand for long-term durability of concrete structures has increased worldwide. This long-term durability demand requires concrete with low permeability, since it has been shown in the literature that there is a direct relationship between permeability and durability. These two major facts have led to the development of high-performance concrete (HPC), which possesses high workability, high strength and low permeability. Producing concrete with low permeability and consequently long-term durability has become more important than attaining a higher strength in most field applications (Aitcin et al., 1990).

These days, high-strength concrete and HPC are commonly used throughout the world and it is necessary to reduce the water/binder ratio to produce them. As a part of this concrete, superplasticizers are used to achieve the required workability; however, because low porosity and permeability are desired, different types of cement replacement materials are usually added to this concrete. According to Aitcin (Neville & Aïtcin, 1998), "what was known as high-strength concrete in the late 1970s is now referred to as HPC, because it is much more than simply stronger".

The partial replacement of cement with SCMs, such as silica fume (Borosnyói, 2016; Muhit, Ahmed, Zaman and Ullah, 2018; Shi et al., 2015), decreases the permeability by the formation of C-S-H gel in the concrete mix, which further puts resistance against corrosion (Malhotra & Mehta, 1996; Report, 1988). Silica Fume (SF) is considered to produce low-permeability concrete because of its high pozzolanicity and extreme fineness (Hou & Chung, 2000). Moreover, the incorporation of SCMs, such as silica fume, tends to fill the spaces between cement grains, decrease water permeability, reduce chloride ion penetration and consequently, reduce the rate of corrosion of reinforcements (Jayaseelan, 2019; Mejía de Gutiérrez, 2003).

Calcium hydroxides produced by the hydration of ordinary Portland cement are consumed by the oxides (SiO_2) present in SF during the pozzolanic reaction, which further results in lower porosity, permeability and bleeding. The pozzolanic reactions also lead to lower heat liberation and strength development, time-consuming activity and smaller pore size distribution. SF, due to its pozzolanic action, improves the bond between the paste and aggregate. So, its use in HPC is widely accepted. The denseness in the concrete mix after incorporation of SF at low water-binder ratio is improved and subsequently compressive, flexural and split tensile strengths are increased (Alexander & Magee, 1999; Alsharie & Alayed, 2019; Bhanja & Sengupta, 2005). Therefore, it has been used as a replacement material in the production of HPC. The same has been observed during an extensive experimental study over water-binder ratios ranging from 0.26 to 0.42 and SF to binder ratios from 0.0 to 0.3 (Bhanja & Sengupta, 2005).

One of the deciding factors controlling the permeability of cement paste is water to binder ratio (w/b) (CEB, 1997; Neville & Brooks, 2010; Rattanashotinunt, Tangchirapat, Jaturapitakkul, Cheewaket & Chindaprasirt, 2018), as it controls the de-percolation of pore structure by determining the initial space between the un-hydrated cement and porosity (Powers, Copeland & Mann, 1959). The pozzolanic property of SF helps in the formation of C-S-H gel and as a result, there is a significant improvement in impermeability. However, other properties, such as workability, get reduced (Khayat, Vachon & Lanctôt, 1997). 15 to 20 mm slump loss as compared to conventional concrete after addition of 7.5% SF has been reported (Ghafoori & Diawara, 2007).

The dispersive action of flocculated cement particles takes place due to the combined effect of superplasticizer and SF (Duval & Kadri, 1998). This was attributed to the fact that during the first minutes of mixing, the superplasticizer is adsorbed by the C_3A phase and interferes with the early hydration of ettringite and C-S-H (Alkaysi, El-Tawil, Liu & Hansen, 2016; Du, Du & Liu, 2014).

Recently, the investigation of non-destructive testing techniques is a very popular subject (Jobli, Hampden & Tawie, 2017; Tsioulou, Lampropoulos & Paschalis, 2017) and the ultrasonic method is one of the non-destructive testing techniques and is frequently adopted for evaluating the quality of *in situ* concrete structures. It can measure the speed of the wave through materials to predict material strength, calculate low-strain elastic

modulus or detect the presence of internal flaws, such as cracking, voids, honeycomb, decay and other damages. The application of Ultrasonic Pulse Velocity (UPV) to the non-destructive evaluation of normal-strength concrete (≤ 41 MPa) quality has been widely investigated for decades (Khan, S. R. M., Noorzaei, J., Kadir, M. R. A., Waleed, A. M. T. and Jaafar, 2007). Also, many authors have studied how UPV can be correlated with concrete strength. A few authors have conducted a comprehensive study of their contributions (Lin, Lai & Yen, 2003).

This paper presents the statistical evaluation of the experimental results obtained to study the combined effect of w/b ratio and SF on water permeability and strength characteristic of HPC. The scope also includes the statistical modeling of test results obtained for the permeability of high-strength concrete (HSC) with SF. Furthermore, a straightforward translation of the derived statistical models into contour diagrams has been developed.

MATERIALS AND METHODS

Materials

In this study, the cement used was ordinary 43 grade Portland cement of (IS: 8112, 1989). SF was used in its dry densified form. It contains (85-98%) amorphous glassy silicon dioxide in the form of microscopic spherical particles. The average diameter of these particles is in the range of 0.1 to 0.15 micrometres, with a specific gravity of 2.2.

X-ray diffraction (XRD) is used for identifying minerals and other crystalline phases in a wide range of materials, particularly where the individual particles are too small to be constantly distinguished by minuscule methods. The data obtained from XRD is used to evaluate the quantitative analysis of the samples to find their chemical compositions.

Cu Ka radiation was used during the XRD analysis of powdered samples of SF and OPC43. At a counting time of 2 s per step and with an increment of 0.05°, scans were run from 10° to 80° for SF and from 10° to 70° for OPC43. Based on the data obtained through XRD, quantitative analysis of the specimens was carried out by plotting graphs and comparing them with the JCPDS charts using the X'pert High score (Plus) software.

Crystallography of Silica Fume (SF) and ordinary Portland cement is shown in Fig 1. The XRD outline of Portland cement shows peaks comparable to Tricalcium Silicate (alite) (C_3S), Dicalcium Silicate (belite) (C_2S), Tricalcium Aluminate (C_3A) and Tetracalcium Aluminoferrite (C_4AF) or brownmillerite. A similar investigation was done for SF with XRD. The XRD pattern of SF, when compared with the JCPDS chart (01-086-2328), shows maximum peaks at 30.4° similar to SiO_2 as a main component of SF. XRD pattern of SF was found to exhibit generally amorphous characteristics.

Fig 2 demonstrates the distribution of grain size for all cementitious materials used in the experimental method. From the figure, it can be observed that OPC and SF particle size distribution is very similar and is smaller than 80 μm. By further observation, it can be seen that SF is slightly finer and this fineness of SF is expected to improve particle packing and may reduce porosity. Table 1 and Table 2 present the physical properties of cement and SF.

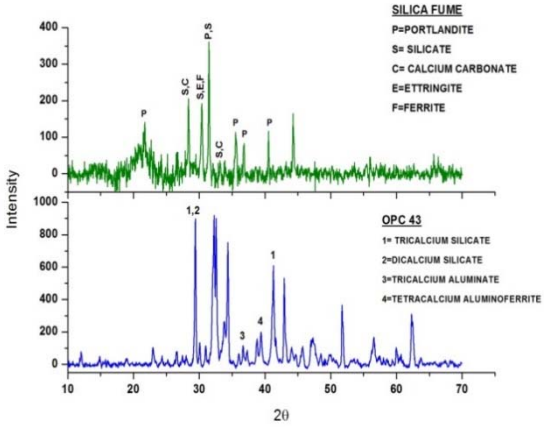

Figure (1): XRD traces of OPC and SF

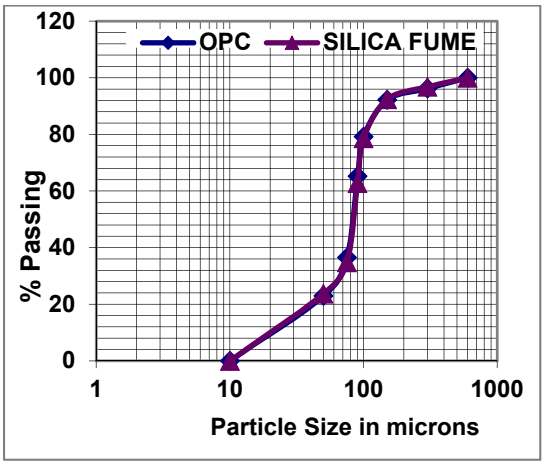

Figure (2): Particle size distribution of cementitious materials

Table 1. Physical properties of 43 grade cement (OPC)

Particulars	Results obtained
Fineness: specific surface (air permeability test) (cm^2/kg)	2250
Normal consistency	30%
Vicat's time of setting (min)	
Initial	48
Final	220
Compressive strength (MPa)	
7-day	34.7
28-day	51.2
Specific gravity	3.15

Table 2. Physical properties of SF (Elkem)

Sl. No.	Parameter	Analysis
1	>45	1.13
2	Pozz. activity index (7d)	132
3	Specific surface	19.4
4	Bulk density	616
5	Specific gravity	2.21

The coarse aggregate used was crushed stone from Pakur sieved to obtain a 20-mm maximum size. After grading, the aggregate was dried under laboratory conditions. The fine aggregate with a 2.6 fineness modulus was natural sand with a Zone- 3 grading. The particle size distribution curve of fine aggregate is shown in Fig 3. The specific gravity and water absorption of the coarse and fine aggregates were 2.86 and 0.70% and 2.66 and 1.35%, respectively.

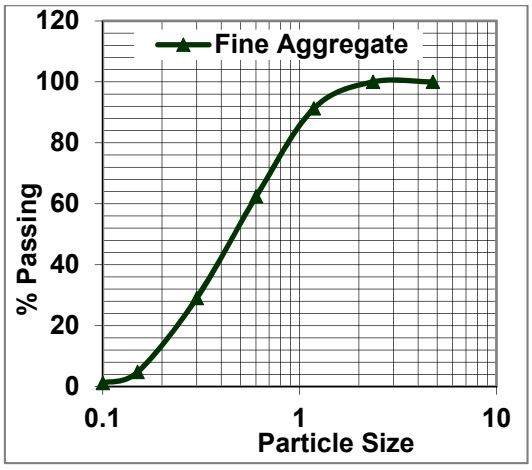

Figure (3): Particle size distribution of fine aggregate

Test Methods

The prepared concrete cube specimens (15 cm) were tested for compressive strength after the curing period of 28 days in accordance with Indian Standard (IS: 516, 1959). Average of three cubes was taken in this investigation.

Standard codes (ASTM C143/C143M, 2015; IS: 1199, 1959) were used to assess the workability of the fresh concrete with the help of the traditional slump test method.

The pulse velocity test was conducted in accordance with the requirements of standard codes (ASTM C597, 2016; IS:13311 (Part-1), 1992). The ultrasonic pulse passing through the concrete was generated by a transducer serving as a transmitter held close to the surface of the concrete specimen. The onset of the pulse on the opposite face of the specimen was detected by another transducer that served as a receiver. This direct transmission method was adopted in this study, because the maximum energy of the pulse was directed at the receiver and the noise to signal ratio could be minimized. Repeated measurements were taken at each transducer arrangement, so that the consistency and accuracy of the UPV measurements were assured. The transmitter and receiver locations were also carefully marked, so that repeated measurements could be taken from the same place. Longitudinal UPV is given by:

$V=L/T$ (km/s) ……..…… ..…..(1)

where

L= travel distance of the wave (m).

T= transit time of the pulse (sec).

The permeability of the concrete cubes of different mix proportions was measured following the guidelines of (IS:3085, 1965). Concrete permeability test apparatus (AIM-381) manufactured by Aimil, Ltd. has been used. In this test, the concrete specimen (15cm×15cm×15cm) is placed in a specially designed cell and hydrostatic pressure is given from one side. The quantity of water percolating through the specimen in a given interval of time is measured. The permeability cell assembly is maintained at the hydrostatic pressure of 12 kg/cm^2. Permeability test was continued for about 24 hours and the outflow considered was an average of all the outflows measured during 24 hours. The side of each specimen was sealed with moisture-insensitive epoxy to prevent water leakage. The coefficient of permeability is

calculated as follows:

$$k = \frac{q}{at\frac{h}{l}} \ldots\ldots \quad \ldots\ldots\ldots\ldots\ldots\ldots\ldots\ldots\ldots\ldots\ldots\ldots (2)$$

where

k = coefficient of permeability in cm/sec.

q = quantity of water permeability uniformly after the steady-state has been reached (mm).

a = area of the face of the specimen in cm^2.

t = time in seconds.

$\frac{h}{l}$ = ratio of the pressure head to the thickness of the specimen.

Experimental Program and Statistical Analysis of Data

Twenty-four control mixes were prepared with partial replacement of cement with SF. All one hundred and forty-four cube specimens of grade M60 concrete with six different weight percentages of SF (0%, 2%, 4%, 6%, 8% and 10%) were cast at various w/b ratios. Properties, such as workability, compressive strength, permeability and UPV, were tested to find the effects of w/b and SF in high-strength concrete. Chemical admixture (ORAMIX-300 of polycarboxylic base) was also used to attain the desirable properties, such as workability. The Indian standard mix proportioning guideline as indicated in IS 10262:2009 was used for the proportioning of mixes.

The mix proportions of all 24 mixes are presented in Table 3. Table 4 depicts the test results in terms of strength, UPV and coefficient of permeability as a non-dimensional parameter for all the mixes. The result of strength accurate to the second decimal place has been presented, while the coefficient of permeability is accurate to four decimal places. To examine the relationship between compressive strength and permeability or UPV and permeability, a set of 20 experimental data was selected omitting all the four reference mixes. Analysis of variance (ANOVA) was used to examine the significance of the factors considered for the development of the strength and permeability prediction model and subsequently to fit an empirical model for permeability and compressive strength. Statistical models were developed through multiple regression analysis using MINITAB (Minitab, 2000) software.

Table 3. Mixture proportions

% SF	w/b	C (kg)	SF (kg)	W (kg)	FA (kg)	CA (kg)	HRWR (lit)
0	0.32	438	0	136.56	822	1066	7.8
2		429	9	136.56	819	1066	7.8
4		420	18	136.56	815	1066	7.8
6		411	27	136.56	812	1066	7.8
8		403	35	136.56	809	1066	7.8
10		394	44	136.56	807	1066	7.8
0	0.36	390	0	137.28	862	1066	7
2		382	8	137.28	859	1066	7
4		374	16	137.28	857	1066	7
6		366	24	137.28	854	1066	7
8		358	32	137.28	851	1066	7
10		351	39	137.28	848	1066	7
0	0.38	370	0	137.56	880	1066	6.6
2		362	8	137.56	877	1066	6.6
4		355	15	137.56	875	1066	6.6
6		347	23	137.56	872	1066	6.6
8		340	30	137.56	869	1066	6.6
10		333	37	137.56	867	1066	6.6
0	0.4	350	0	137.8	896	1066	6.25
2		343	7	137.8	894	1066	6.25
4		336	14	137.8	891	1066	6.25
6		329	21	137.8	889	1066	6.25
8		322	28	137.8	886	1066	6.25
10		315	35	137.8	884	1066	6.25

Table 4. 28-day test results

%SF	w/b	f_{ck} (MPa)	UPV(m/sec)	K_{sf}/K_o	log (K_{sf}/K_o)
0	0.32	70.82	5248	1.0000	0.0000
2	0.32	72.96	5457	0.0474	-1.3244
4	0.32	73.74	5688	0.0224	-1.6500
6	0.32	74.26	5946	0.0031	-2.5126
8	0.32	74.89	6379	0.0014	-2.8393
10	0.32	74.62	6500	0.0010	-2.9935
0	036	68.71	4998	1.0000	0.0000
2	0.36	69.87	5046	0.0670	-1.1736
4	0.36	70.98	5288	0.0484	-1.3151
6	0.36	71.25	5467	0.0178	-1.7491
8	0.36	73.12	5798	0.0087	-2.0612
10	0.36	72.74	5889	0.0027	-2.5768
0	0.38	67.67	4767	1.0000	0.0000
2	0.38	68.11	4859	0.0830	-1.0810
4	0.38	69.37	5071	0.0572	-1.2425
6	0.38	69.58	5201	0.0248	-1.6056
8	0.38	71.92	5488	0.0118	-1.9265
10	0.38	71.57	5571	0.0040	-2.4022
0	0.4	65.93	4466	1.0000	0.0000
2	0.4	66.21	4578	0.0976	-1.0105
4	0.4	67.48	4798	0.0685	-1.1645
6	0.4	67.77	4926	0.0302	-1.5206
8	0.4	70.53	5119	0.0142	-1.8491
10	0.4	70.16	5196	0.0081	-2.0893

RESULTS AND DISCUSSION

The statistical summary of f_{ck} by % SF is presented in Table 5. The statistical summary indicates that the means and standard deviations do not appear to differ. The standard deviations of the five sets of experiments varied between 1.84 and 2.86. The overall standard deviation indicated good control over the production of the HSC specimens.

Table 5. Statistical summary of f_{ck} by % SF

% SF	N	Mean	St. Dev.	Min.	Median	Max.	Normality Test	
							P	Decision
2	4	69.287	2.8685	66.21	68.99	72.96	0.798	Pass
4	4	70.392	2.6507	67.48	70.18	73.74	0.828	Pass
6	4	70.715	2.7577	67.77	70.42	74.26	0.789	Pass
8	4	72.615	1.8494	70.53	72.52	74.89	0.857	Pass
10	4	72.273	1.8873	70.16	72.16	74.62	0.849	Pass

Slump Test Results

Figure 4 shows the outcome of the slump test for various w / b ratios and different percentages of SF. From the graph shown, it can be concluded that a high slump value for w/b=0.4 was achieved. However, at a lower water-cement ratio, the slump value gets reduced for the same SF replacement level.

The water content in the mix is partly used in hydration and partly in imparting workability. Hence, as the water to binder ratio reduces, water in the cementitious mix reduces and as a result, workability reduces. However, HRWR with active solid is used to disperse the cementitious material to compensate for the loss in workability. Further, after the addition of SF, the concrete mix becomes more cohesive. In small dosages, it put resistance in segregation. The extra dosage of SF makes the concrete sticky, as the extra SF which is not utilized to capture free lime becomes flocculated.

The potential water-reducing effect of superplasticizer and SF is counterbalanced by utilizing a

high content of SF which consequently results in lowered workability. This very much seems to recommend that for decreased water demand and high workability, there must be an optimum SF content which will give the most extreme scattering of cement and SF. Above this optimum level, there will be an increase in water demand, resulting in lower workability due to the very superior fineness of SF.

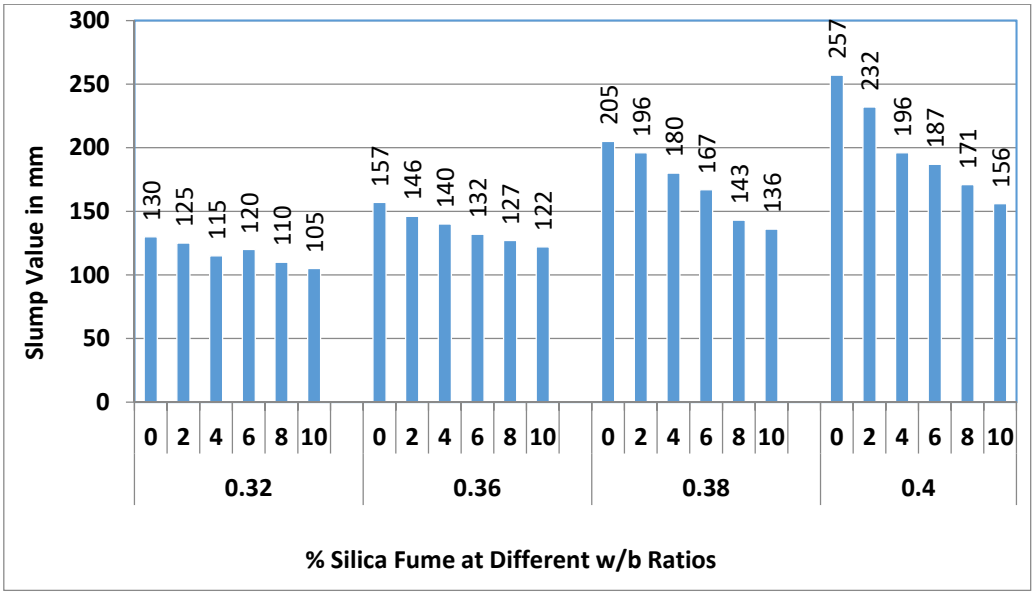

Figure (4): Effect of w/b ratio and SF on slump value

Compressive Strength Test

Cube specimens prepared for compressive strength testing were tested in the laboratory and different crushing strength values were found. Table 4 gives the overall picture of variation in compressive strength for different w/b ratios with varying percentages of SF. The overall strength varied from 65.93 N/mm^2 to 74.89 N/mm^2. From Table 4, it can be concluded that compressive strength increases with an increase in SF content for the same w/b ratio. From the figure, it can also be inferred that the strength achieved at a 10% replacement level of SF is less as compared to the strength achieved at an 8% replacement level of SF. However, the percentage decrease was assessed to be less than 1%.

A basic law in concrete technology states that the strength of concrete (or mortar) is inversely related to the water/cement (w/c) ratio. This relationship is changed quantitatively, but not qualitatively, when another cementitious material is added. From Fig 5, it can be concluded that for the same replacement level of SF, compressive strength is inversely proportional to w/b ratio. Further, for a fixed percentage of SF, it is observed that there is a shift in the strength *vs.* w/b curve to a higher level, but the shape of the curve is maintained. Fig. 6 illustrates this point for the 28-day strength of HSC with varying percentages of SF. For a given SF content, the points show no systematic deviation from a common curve.

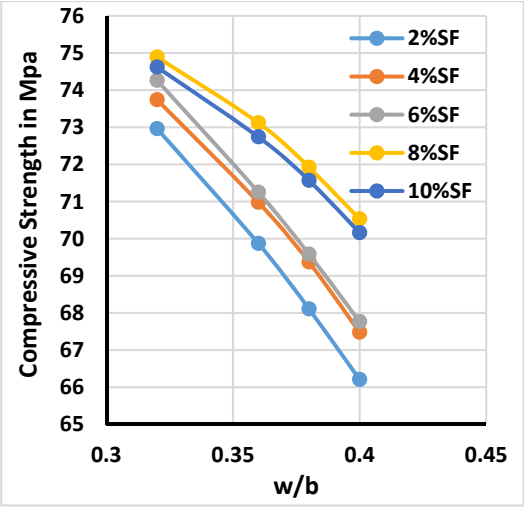

Figure (5): Effect of w/b ratio on compressive strength test results

Statistical Analysis of Data and Fitting of the Compressive Strength Model

Multiple regression is an examination of the linear relationship between one continuous response and two

or more predictors. To think about the incremental effect of the two parameters at the same time on compressive quality, multiple regression was performed on a set of 20 experimental data for compressive strength. To predict the compressive strength of HSC with SF, a numerical algorithm was developed through multiple regression analysis and is given in Equation (3).

$$f_{ck} = 103.11 - 1.075 \times (\%SF) - 94.55 \times \left(\frac{w}{b}\right) + 4.07 \times \left(\%SF \times \frac{w}{b}\right) \ldots\ldots\ldots\ldots\ldots \quad \ldots(3)$$

The model of compressive strength (Eq. (3)) indicated that both the *w/b* and SF content had an impact. Indeed, the established model indicates that the *w/b* had an impact approximately four times greater than that of the SF content on the compressive strength of concrete.

At 90% confidence interval, the model equation can explain 96.13% of the variations in compressive strength. Further, the relationship between the response and the variable is statistically significant at 90% confidence interval.

Ultrasonic Pulse Velocity (UPV)

The basic principle of evaluating the quality of concrete by UPV measurement is that comparatively higher velocities are obtained when the quality of concrete is better in terms of homogeneity, density and uniformity. Lower velocities are obtained in the case of poorer quality. From the results obtained (Table 4), the pulse velocity of all concrete mixes after 28 days was > 4.5 km/sec, indicating that the quality of concrete mixes was excellent and that mixes were homogeneous as per (IS:13311 (Part-1), 1992).

From Table 4, it can be observed that lower longitudinal velocity values were obtained in case of mixes with higher w/b ratio. This may be due to the voids in the concrete matrix which may have attenuated the pulse strength. The scatter plot of the UPV *versus* w/b ratio (Fig. 6) shows that the pulse velocity is inversely proportional to the w/b ratio. However, the pulse velocity increases with the increase in SF content. The results demonstrated in Table 4 indicate an increase in pulse velocity at all replacement levels of cement by SF and consequently increases in compressive strength and dynamic modulus. This may be due to the development of a dense internal structure in the concrete matrix. The significant improvement in UPV indicates that after addition of HRWR and SF, the air entrainment was further reduced.

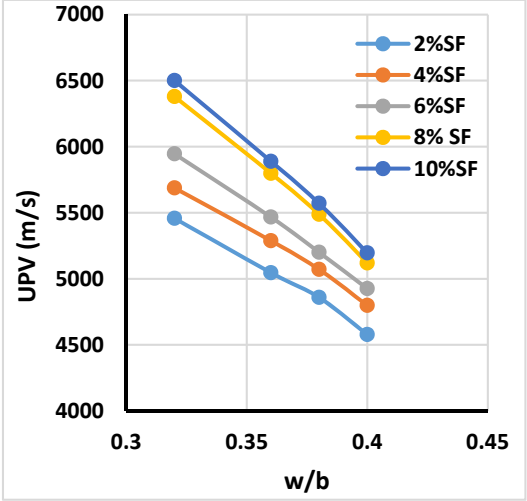

Figure (6): Scatter plot of UPV *versus* w/b ratio

Water Permeability Test

Cube specimens of concrete prepared for permeability were tested in the laboratory at a curing age of 28 days and the coefficient of permeability was found for each sample by calculation as previously described. The values of the coefficient of permeability of each cube containing a different percentage of SF by weight are shown in Table 4. The ratio of permeability (K_{sf}/K_o) is defined as "the permeability of concrete containing pozzolanic materials divided by the permeability of OPC concrete at the same age of testing".

Permeability *versus* % Silica Replacement

The effect of SF incorporation on the permeability ratio of concrete at 28 days has been graphically represented in Fig 7. From Fig 7, it can be seen that the incorporation of SF in concrete reduces the coefficient of permeability by a good amount for the same w/b ratio. The reduction in coefficient of permeability is maximum at 10% SF replacement. This may be attributed to the fact that SF not only improves the pore structure in cement mortar, but also improves the interface between cement mortar and aggregate (Torii, 1994). Further, because of its microfiller and pozzolanic influences, SF makes the transition zone of the cement mortar homogeneous and dense, thereby enhancing the permeability resistance (Armaghani, M. and Larsen, T., 1992; Banthia & Mindess, 1989; Duan, Yan, Zhou, Luo & Shen, 2015; Ping & Beaudoin, 1992; Torii, K., 1994).

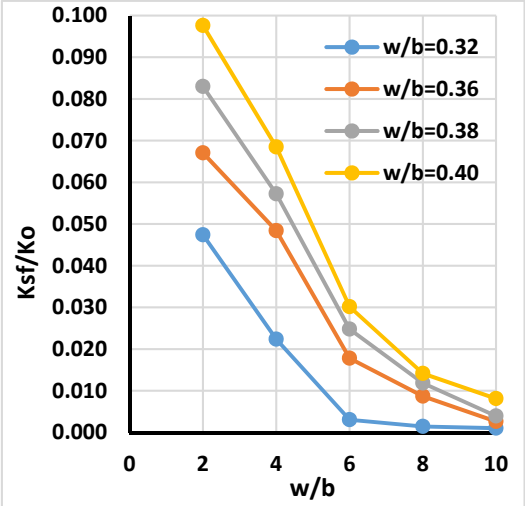

Figure (7): Effect of w/b ratio and % SF on K_{sf}/ K_o

Permeability *versus* w/b Ratio

Fig. 8 represents the effect of w/b ratio on the permeability of HSC with SF. The reduction in w/b ratio considerably reduces the permeability coefficient of the mixes at the same SF replacement level. A decreasing percentage of SF results in a shift of the K_{sf}/ K_o *vs.* w/b curve to a higher level, indicating an increase in permeability. It has been identified in previous research that the w/b ratio has a significant influence on permeability (Goto & Roy, 1981).

Statistical Analysis of Data and Fitting of the Coefficient of Permeability Model

To study the synergistic impact of two variables on K_{sf}/K_o, multiple regression was performed for K_{sf}/K_o. The interaction plot for K_{sf}/K_o shown in Fig 9 describes how K_{sf}/K_o changes if the settings of w/b or % SF are varied. It can be seen here that SF has a significant impact on permeability as compared to w/b ratio. The numerical algorithm so developed to predict the K_{sf}/ K_o is given in Equation 4.

$$K_{sf} / K_0 = -0.1802 + 0.00571 \times \%SF + 0.8076 \times w / b + 0.001059 \times (\%SF)^2 - 0.07509 \times \%SF \times w / b \ldots\ldots \quad \ldots(4)$$

At a 90% confidence interval (CI), the model equation can explain 98.83% of the variation in K_{sf}/ K_o. Further, to evaluate the precision of the proposed model, normal probability plot of the residuals or the error terms has been plotted. This chart plots the residuals *versus* their expected values when the dissemination is normal. The residuals from the examination ought to be regularly disseminated. Practically speaking, for adjusted or almost adjusted designs or for data with an extensive number of perceptions, moderate departures from normality don't truly influence the outcomes. The normal probability plot of the residuals should roughly follow a straight line. The normal probability plot surveys the normality of residuals in small datasets. The normal probability plots shown in Fig. 10 – Fig. 12 indicate good accuracy for the established model, as the residuals are normally distributed.

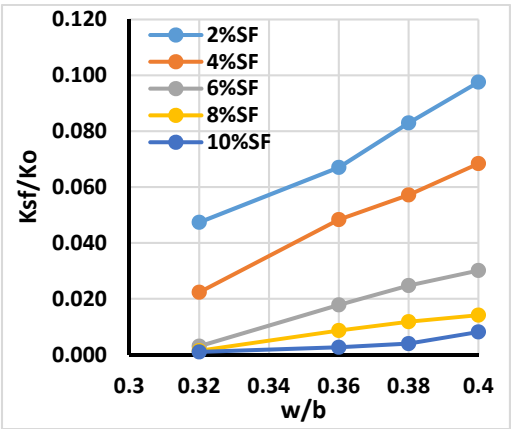

Figure (8): Effect of w/b ratio and %SF on K_{sf}/ K_o

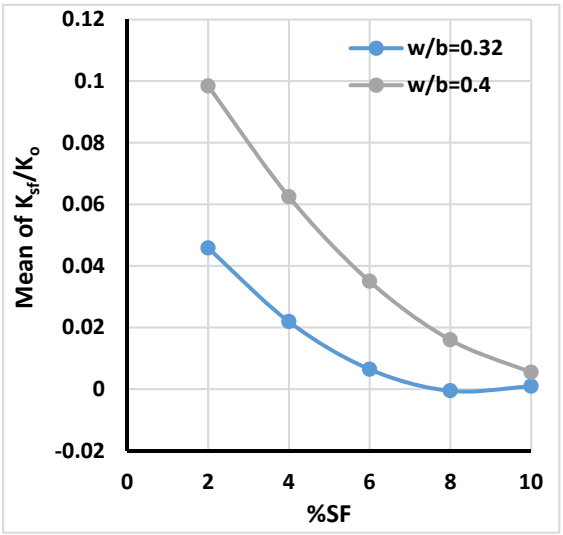

Figure (9): Interaction plots for K_{sf}/K_o

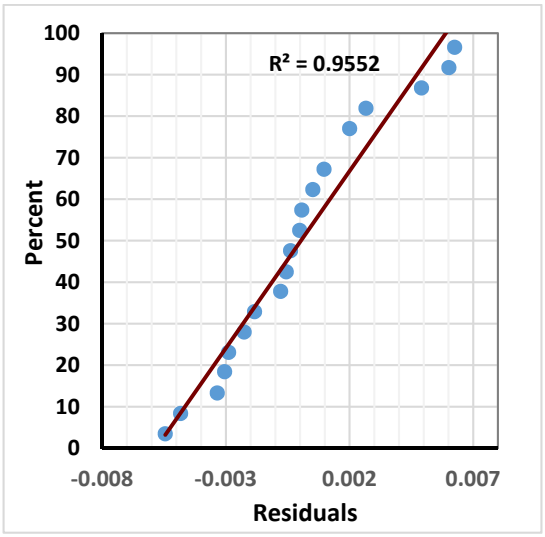

Figure (10): Normal probability plot

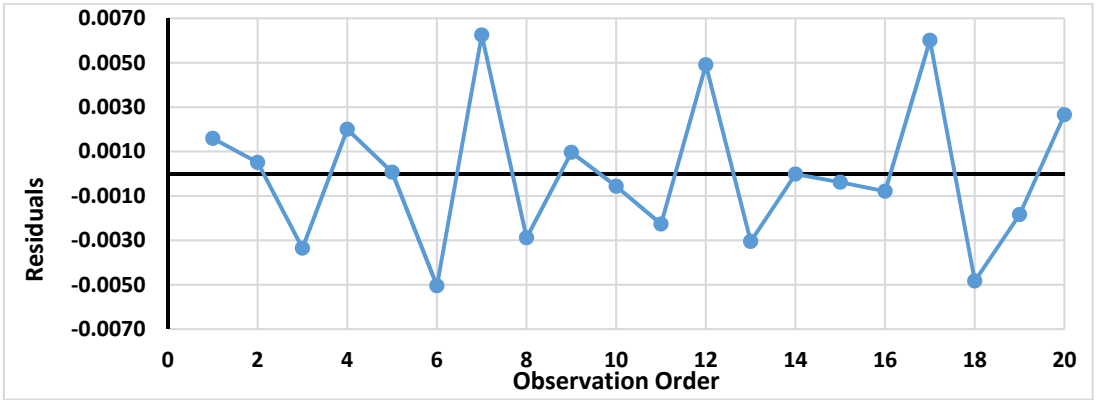

Figure (11): Residual plots for K_{sf}/K_o

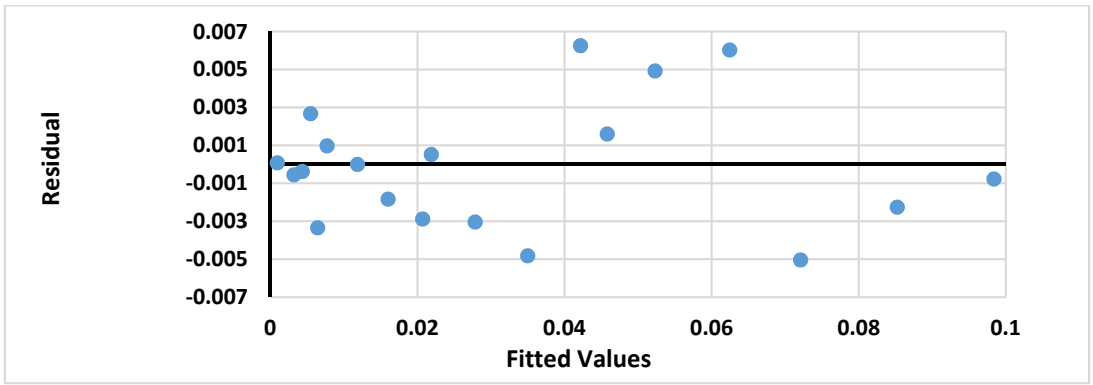

Figure (12): Residual *versus* fits for K_{sf}/K_o

Permeability *versus* Strength

Concrete in practice is specified by strength. Fig. 13 illustrates the relationship between water permeability and compressive strength. There is a relationship, with the permeability logarithmically decreasing as the strength increases. Less R^2 value, however, implies that a strength calculation alone cannot infer the water permeability coefficient and therefore, the durability of concrete.

Permeability *versus* UPV

The relationship between water permeability and UPV is illustrated in Fig. 14. Previous studies have shown that there is a good correlation between UPV and

compressive strength. However, no clear rules have been presented in the literature to describe how the relationship between UPV and permeability coefficient of concrete changes with its mix proportions. Fig. 14 shows that just like for permeability *versus* strength, a logarithmic relationship with a high correlation coefficient ($R^2 = 0.79$) exists. From the figure, it can be again inferred that the permeability reduces logarithmically as the pulse velocity increases.

The propagation of ultrasonic wave largely depends upon the denseness of the medium. So, the higher the value of UPV, the higher the denseness. Further, the cube compressive strength depends mainly upon the matrix of the concrete mix instead of its compactness. This is evident from the fact that high R^2 value is obtained for permeability *versus* UPV as compared to permeability *versus* strength for the same regression fit.

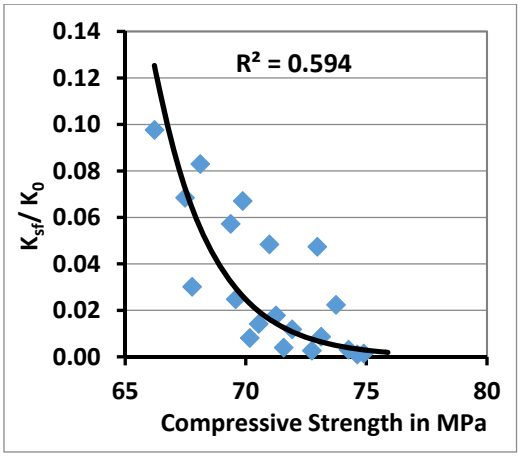

Figure (13): Compressive strength *vs.* k_{sf}/k_0

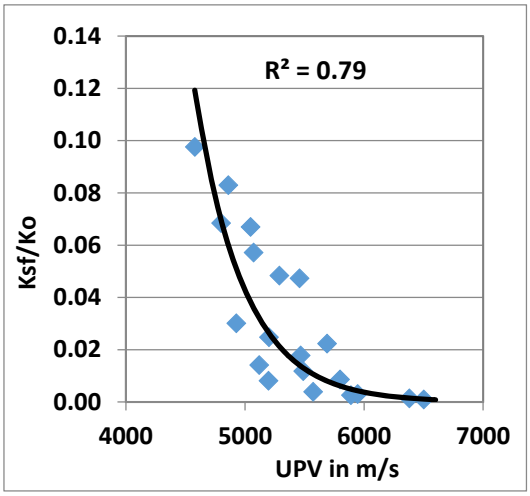

Figure (14): UPV *vs.* k_{sf}/k_0

Correlation Model for Log_{10} (K_{sf}/K_o) with Strength and UPV

Impermeability of concrete enhances its durability, so an indirect measurement of the coefficient of permeability through UPV and strength can be utilized to assess the durability of concrete. From Fig. 13 and Fig. 14, it has been established that the non-dimensional parameter (K_{sf}/K_o) varies logarithmically with both compressive strength and UPV. Hence, an attempt has been made to correlate Log_{10} (K_{sf}/K_o) with strength and UPV. To identify the interactive and individual effects of variable factors on the dependent variable, analysis of variance (ANOVA) was carried out. ANOVA of the test results in the present study was carried out with the software named MINITAB (Minitab, 2000). The regression model for the $Log_{10}(K_{sf}/K_o)$ was obtained based on the ANOVA results. The ANOVA results are presented in Table 6. If the P-value was found to be less than 0.05 (95% confidence level), a factor was assumed to have a major impact on the compressive strength. The P-value was derived from Fisher's distribution table.

Table 6. Analysis of variance (ANOVA) results

Source	DF	Adj. SS	Adj. MS	F-Value	P-Value
Regression	2	5.804	2.902	41.32	0.000
f_{ck}	1	0.298	0.297	4.24	0.055
UPV	1	1.647	1.647	23.45	0.000

The polynomial regression model obtained for Log_{10} (K_{sf}/K_o) using the data presented in Table 4 is presented as follows:

$$\log_{10}(K_{sf}/K_0) = -3.08 + 0.1523 \times f_{ck} - 0.001763 \times UPV \quad ...(5)$$

The model summary is presented in Table 7. The normal probability plot shown in Fig. 15 indicates good accuracy for the established model, as the residuals are normally distributed.

Table 7. Model summary

S	R-sq.	R-sq. (adj.)	R-sq. (pred.)
0.265002	82.94%	80.93%	77.14%

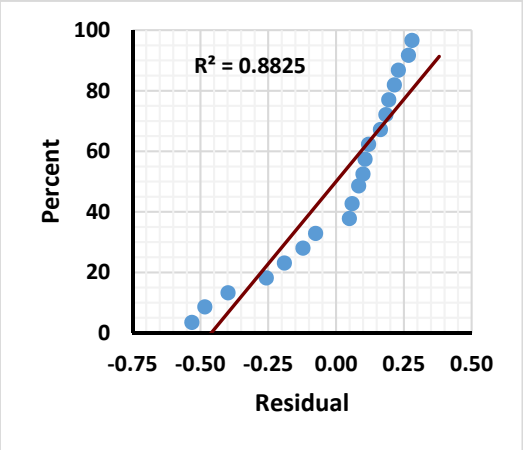

Figure (15): Normal probability Plot for Log_{10} (K_{sf}/K_o)

Use of Established Models

Contour diagrams were set up as a straightforward translation of the derived statistical models. The contour diagrams were utilized to look at the exchange between the impacts of the distinctive parameters (*w*/*b* and %SF) on the thought about responses. Two-dimensional contour charts were developed to show how the responses (compressive strength and permeability coefficient ratio) changed with variations in the *w*/*b* and % SF (Figs. 16-18). Fig. 18 shows how the log of non-dimensional parameter K_{sf}/K_o changes with variations in compressive strength and UPV.

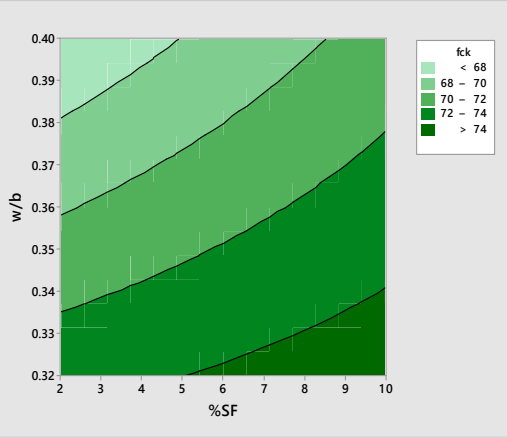

Figure (16): Contour plot of f_{ck} *vs.* w/b, %SF

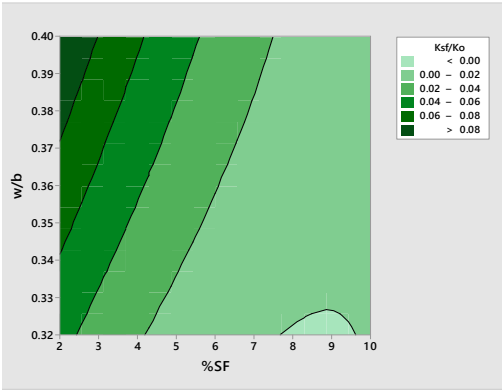

Figure (17): Contour plot of K_{sf}/K_o *vs.* w/c, %SF

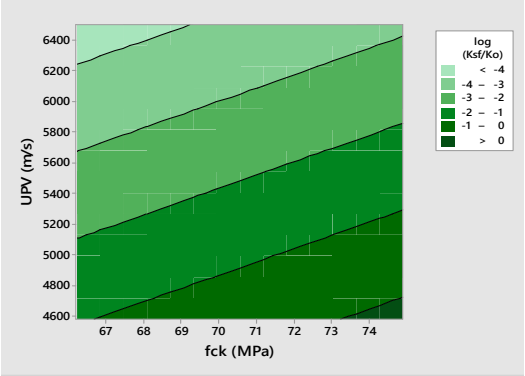

Figure (18): Contour plot of log_{10} (K_{sf}/K_o) *vs.* UPV, f_{ck}

CONCLUSIONS

This study led to the following conclusions:

1. SF has a significant influence on the water permeability and mechanical properties of concrete.
2. At any replacement level of SF, the strength decreases with the increase in the water to binder ratio of 0.36, beyond which a sharp reduction was observed, thus obeying Abrams' law.
3. Regardless of the *w*/*b*, the compressive strength increased with SF replacement percentage up to 8% and thereafter there was a reduction trend as the SF content increased and thus, the compressive strength of HSC can be optimized by using 8% SF replacement by weight of cement.
4. Statistical relationships between the compressive strength of HPC, *w*/*b* and SF are developed. The empirical relations developed by the multiple regression method can serve as a valuable engineering tool for predicting permeability and strength. It is convenient and easy to use these models for numerical experiments to review.

5. From the contour plots, it can be established that almost impermeable HSC can be achieved with w/b ratio of less than 0.33 and SF percentage between 7% and 9%.
6. From the contour plots, it is further established that for higher contour value, UPV is more as compared to compressive strength.
7. Since the relations are empirical, they are valid for the materials and the range of variables studied herein, yet this approach can be useful for developing relations that are of practical use for engineers based on a relatively small number of tests.

REFERENCES

Aitcin, P. C., Sarkar, S. L., and Laplante, P. (1990). "Long-term characteristics of a very high-strength concrete." Concrete International: Design and Construction, 12 (1), 40-44.

Alexander, M. G., and Magee, B. J. (1999). "Durability performance of concrete containing condensed silica fume." Cement and Concrete Research, 29 (6), 917-922.

Alkaysi, M., El-Tawil, S., Liu, Z., and Hansen, W. (2016). "Effects of silica powder and cement type on durability of ultra-high-performance concrete (UHPC)." Cement and Concrete Composites.

Alsharie, H., and Alayed, O. (2019). "The effect of replacing fine silica with stone cuttings' powder on the compressive strength of concrete: A case study in Jordan." Jordan Journal of Civil Engineering, 13 (1), 124-135.

Armaghani, M., Larsen T., and R.D. (1992). "Aspects of concrete strength and durability". Transportation Research Record No. 1335. Transportation Research Board, National Research Council, Washington, DC.

ASTM C143/C143M. (2015). "Standard test method for slump of hydraulic-cement concrete".

ASTM C597. (2016). "Standard test method for pulse velocity through concrete." American Society for Testing and Materials, West Conshohocken, PA, USA.

Banthia, N., and Mindess, S. (1989). "Water permeability of cement paste." Cement and Concrete Research, 19 (c), 727-736.

Bentz, D. P., Ehlen, M.A., Ferraris, C. F., and Garboczi, E. J. (2001). "Sorptivity-based service life predictions for concrete pavements." 7th International Conference on Concrete Pavements–Orlando, Florida, USA, Sept., 1, 9-13. Retrieved from: http://citeseerx.ist.psu.edu/viewdoc/download?doi=10.1.1.23.8113&rep=rep1&type=pdf

Bhanja, S., and Sengupta, B. (2005). "Influence of silica fume on the tensile strength of concrete." Cement and Concrete Research, 35 (4), 743-747.

Borosnyói, A. (2016). "Long-term durability performance and mechanical properties of high-performance concretes with combined use of supplementary cementing materials." Construction and Building Materials.

CEB, C. E.-I. (1997). "Durable concrete structures." London: Thomas Terford.

Chia, K. S., and Zhang, M. H. (2002). "Water permeability and chloride penetrability of high-strength lightweight aggregate concrete." Cement and Concrete Research, 32(4), 639–645.

Du, H., Du, S., and Liu, X. (2014). "Durability performances of concrete with nano-silica." Construction and Building Materials.

Duan, P., Yan, C., Zhou, W., Luo, W., and Shen, C. (2015). "An investigation of the microstructure and durability of a fluidized bed fly ash-metakaolin geopolymer after heat and acid exposure." Materials and Design, 74, 125-137.

Duval, R., and Kadri, E. H. (1998). "Influence of silica fume on the workability and the compressive strength of high-performance concretes." Cement and Concrete Research, 28 (4), 533-547.

Ghafoori, N., and Diawara, H. (2007). "Strength and wear resistance of sand-replaced silica fume concrete." ACI Materials Journal, 104 (2), 206-214.

Goto, S., and Roy, D. M. (1981). "The effect of w/c ratio and curing temperature on the permeability of hardened cement paste." Cement and Concrete Research, 11 (4), 575-579.

Hou, J., and Chung, D.D.L. (2000). "Effect of admixtures in concrete on the corrosion resistance of steel reinforced concrete." Corrosion Science, 42 (9), 1489-1507.

IS: 1199. (1959). "Methods of sampling and analysis of concrete." Bureau of Indian Standards.

IS: 516. (1959). “Mrthods of tests for strength of concrete.” Bureau of Indian Standards, New Delhi.

IS: 8112. (1989). “43 grade ordinary Portland cement: Specification.” Bureau of Indian Standards.

IS:13311 (Part-1). (1992). “Non-destructive testing of concrete: Method of testing.” Bureau of Indian Standards.

IS:3085. (1965). “Method of test for permeability of cement mortar and concrete.” Bureau of Indian Standards.

Jayaseelan, R. (2019). “Investigation on the performance characteristics of concrete incorporating nanoparticles.” Jordan Journal of Civil Engineering, 13 (2), 351-360.

Jobli, A. F., Hampden, A. Z., and Tawie, R. (2017). “The role of ultrasonic velocity and Schmidt hammer hardness: The simple and economical non-destructive test for the evaluation of mechanical properties of weathered granite.” In: AIP Conference Proceedings.

Khan, S.R.M., Noorzaei, J., Kadir, M.R.A., Waleed, A.M.T., and Jaafar, M.S. (2007). “UPV method for strength detection of high-performance concrete.” Structural Survey, 25 (1), 61-73.

Khayat, K. H., Vachon, M., and Lanctôt, M. C. (1997). “Use of blended silica fume cement in commercial concrete mixtures.” ACI Materials Journal, 94 (3), 183-192.

Lin, Y., Lai, C. P., and Yen, T. (2003). “Prediction of ultrasonic pulse velocity (UPV) in concrete.” ACI Materials Journal, 100 (1), 21-28.

Malhotra, V.M., and Mehta, P.K. (1996). Pozzolanic and cementitious materials". Advanced Concrete Technology (Vol. 1). Retrieved from: https://books.google.com/books?hl=en&lr=&id=IZs6zne_pAUC&pgis=1

Mejía de Gutiérrez, R. (2003). “Effect of supplementary cementing materials on the concrete corrosion control.” Revista de Metalurgia, 39 (94), 250-255.

Minitab, I. (2000). “MINITAB statistical software.” Minitab Release, 14 (c), 671-673. Retrieved from: https://scholar.google.com/scholar?q=minitab&hl=en&as_sdt=0,15#1

Muhit, I. Bin, Ahmed, S. S., Zaman, M. F., and Ullah, M. S. (2018). “Effects of multiple supplementary cementitious materials on workability and strength of lightweight aggregate concrete.” Jordan Journal of Civil Engineering.

Neville, A., and Aïtcin, P.-C. (1998). “High-performance concrete: An overview.” Materials and Structures, 31 (2), 111-117.

Neville, A.M.M., and Brooks, J.J.J. (2010). “Concrete Technology.” Building and Environment.

Ping, X., and Beaudoin, J. J. (1992). “Modification of transition zone microstructure - silica fume coating of aggregate surfaces.” Cement and Concrete Research, 22 (4), 597-604.

Powers, T. C., Copeland, L. E., and Mann, H. M. (1959). “Capillarity continuity or discontinuity in cement pastes.” J. PCA Research and Development Lab.

Rattanashotinunt, C., Tangchirapat, W., Jaturapitakkul, C., Cheewaket, T., and Chindaprasirt, P. (2018). “Investigation on the strength, chloride migration and water permeability of eco-friendly concretes from industrial by-product materials.” Journal of Cleaner Production.

Report, F. (1988). "Condensed silica fume in concrete". FIP State of Art Report, FIP Commission of Concrete. UK: Thomas Telford House.

Salvoldi, B. G., Beushausen, H., and Alexander, M. G. (2015). “Oxygen permeability of concrete and its relation to carbonation.” Construction and Building Materials, 85, 30-37.

Shi, C., Wu, Z., Xiao, J., Wang, D., Huang, Z., and Fang, Z. (2015). “A review on ultra high-performance concrete: Part I. Raw materials and mixture design.” Construction and Building Materials.

Torii, K.-K.M. (1994). "Mechanical and durability-related properties of high-strength concretes containing silica fume". Report SP-149-26. American Concrete Institute, Detroit.

Tsioulou, O., Lampropoulos, A., and Paschalis, S. (2017). “Combined non-destructive testing (NDT) method for the evaluation of the mechanical characteristics of ultra-high-performance fibre-reinforced concrete (UHPFRC).” Construction and Building Materials.

Zunino, F., and Lopez, M. (2016). “Decoupling the physical and chemical effects of supplementary cementitious materials on strength and permeability: A multi-level approach.” Cement and Concrete Composites, 65, 19-28.